



ISSN: 0067-2904

## Studying the effect of adding a mixture of metal oxides to paraffin wax as solar energy cells and corrosion inhibitors.

Tabarak saad hasan \* Basim Ibrahim Al-Abdaly

Department of Chemistry , College of Science, University of Baghdad, Baghdad , Iraq

Received: 10/9/2023

Accepted: 27/8/2024

Published: 30/9/2025

### ABSTRACT

In this study, nanoparticles of metal oxides (CoO, NiO, and TiO<sub>2</sub>) were synthesized using the hydrothermal method. These nanoparticles were then incorporated into paraffin wax, serving as a matrix, to create nanocomposites. The resulting materials, [TiO<sub>2</sub>; CoO/paraffin] and [TiO<sub>2</sub>; NiO/paraffin], were prepared using ultrasonic techniques. The morphology, size, and structures of the synthesized nanocomposites were examined and characterized using atomic force microscopy (AFM), field emission scanning electron microscopy with energy dispersive spectroscopy (FESEM-EDS), energy dispersive X-ray (EDX), X-ray diffraction (XRD), Fourier transformer infrared (FT-IR), and ultraviolet-visible (UV-Vis) spectroscopy to confirm the design of nanocomposites based nanostructures and reveal their distinctive features from there distribution on paraffin wax. The results of AFM for the two synthesized nanostructures [TiO<sub>2</sub>; CoO/paraffin], [TiO<sub>2</sub>; NiO/paraffin], showed that nanoparticles were in the nanoscale (87.54 nm, and 56.74 nm) respectively. The three-dimensional images depict heterogeneous grooves in all nanostructures of the synthesized composites. This is primarily attributed to the agglomeration of metal oxide nanoparticles, which results in some of the paraffin surface being covered. The activities of nanocomposites synthesized were studied from the industrial side, including solar cell energy and the use of these nanocomposites as inhibitors for corrosion. The findings for all of these nanocomposites revealed they have the properties of solar cells and a significant inhibitory effect.

**Keywords:** paraffin wax ,hydrothermal method ,metal oxide , ultra-sonic method, doping .

تبارك سعد حسن \* باسم ابراهيم العبدلي

جامعة بغداد , كلية العلوم , قسم علوم الكيمياء , بغداد , العراق

### الخلاصة

في هذه الدراسة ، تم تصنيع الجسيمات النانوية لأكاسيد المعادن (CoO و NiO و TiO<sub>2</sub>) باستخدام الطريقة الحرارية المائية. ثم تم دمج هذه الجسيمات النانوية في شمع البارافين ، بمثابة مصفوفة ، لإنشاء مركبات نانوية. المواد الناتجة، [TiO<sub>2</sub>; CoO / البارافين] و [TiO<sub>2</sub>; NiO / البارافين] ، تم تحضيرها باستخدام تقنيات الموجات فوق الصوتية.. تم فحص طيفغرافية وحجم وتركيب المركبات النانوية المركبة وتمييزها باستخدام مجهر القوة الذرية (AFM) والمجهر الإلكتروني الماسح الانبعاث الميداني (FESEM) والأشعة السينية المشتتة للطاقة (EDX) حيود الأشعة السينية (XRD) طيف الأشعة تحت الحمراء FT-IR) والتحليل الطيفي للأشعة فوق البنفسجية المرئية (UV-Vis) من أجل تأكيد تصميم الهياكل النانوية

\*Email: [totasaad929@gmail.com](mailto:totasaad929@gmail.com)

القائمة على المركبات النانوية والكشف عن ميزاتها المميزة من حيث التوزيع على شمع البارافين. نتائج AFM لهيكل النانو المركب  $[CoO / TiO_2]$  لبارافين ،  $[NiO / TiO_2]$  لبارافين ، كان حجم الجسيمات النانوية في المقياس النانوي (87.54 نانومتر ، و 56.74 نانومتر) على التوالي. الصور ثلاثية الأبعاد أخايد غير متجانسة في جميع الهياكل النانوية للمركبات المركبة. ويعزى ذلك في المقام الأول إلى تكتل جسيمات أكسيد المعادن النانوية ، مما يؤدي إلى تغطية بعض سطح البارافين. تمت دراسة أنشطة المركبات النانوية المركبة من الجانب الصناعي ، بما في ذلك طاقة الخلايا الشمسية واستخدام هذه المركبات النانوية كمثبطات للتآكل. كشفت النتائج لجميع هذه المركبات النانوية أن لها خصائص الخلايا الشمسية وتأثير تثبيط كبير .

## 1.Introduction

The term Nanocomposite refers to a composite that contains a phase with a nanoscale morphology, such as nanoparticles, nanotubes, or lamellar nanostructures. Materials that consist of multiple distinct phases are considered multiphase materials. For a substance to be classified as a nanomaterial, at least one of these constituent phases must have a diameter within the range of 10 to 100 nm. Nanocomposites have emerged as beneficial replacements for engineering materials that currently have drawbacks. nano composites can be divided into groups based on the elements of their scattered matrix and dispersion phase [1]. This study experimentally explores an innovative approach to address the worldwide energy challenge by investigating advanced thermal energy storage technology. To enhance the thermal performance of paraffin wax as phase change material (PCM), nanoparticles were utilized at 3% wt. concentration in mono and hybrid form copper oxide (CuO). Nickel oxide nanoparticles have a greater capacity to absorb solar radiation. They are also able to use the thermal energy acquired during the day for distillation at night, thereby increasing productivities through both mechanisms. The salty water in the reservoir is affected by the convection of heat energy that has been absorbed [2, 3]. The concept behind nanocomposite is to develop and make new materials that are remarkably adaptable and improved in physical qualities using building blocks with diameters in the nanoscale range. Among the studied nanomaterials is wax, which was dealt with at the nanoscale level that is supported in the literature [4]. In this study, the researchers aimed to enhance the properties of paraffin wax by incorporating nanometal oxides through a doping process to create new nanocomposite materials. The primary objective was to improve the characteristics of the wax by adding nanometal oxides and evaluating the impact on the surface and structural properties of the wax. The researchers also investigated the potential applications of the modified wax in industrial fields, such as solar cells and corrosion inhibitors.

## 2.Experimental part

### 2.1 Chemicals

Cobalt (II) nitrate hexahydrate  $[Co (NO_3)_2.6H_2O]$ , sodium hydroxide NaOH were purchased from Sigma Aldrich. While nickel (II) nitrate hexahydrate  $[Ni (NO_3)_2.6H_2O]$ , titanium tetra isopropoxide  $Ti(OCH(CH_3)_2)_4$ , isopropanol were supplied from BDH.

### 2.2Methods

#### 2.2.1 Synthesis of cobalt oxide nanoparticles $[CoO]$ by hydrothermal method.

A 2.8gm of  $Co(NO_3)_2.6 H_2O$  (as a precursor) was dissolved in 30 mL of deionized water to make (0.0003 M) solution (1st), and 0.2gm of NaOH was dissolved in 10mL of deionized water to make (0.00005 M) solution (2nd). The two solutions were transferred to a Teflon-lined autoclave cell. The resulting mixture was then heated to approximately 150°C over 12 hours, with a heating rate of 2°C per minute. The cell was cooled and separated by centrifugation at 4000 (rpm) for 10 min. After that, the separated sample was dried at 90°C.

### 2.2.2 Synthesis of Nickel oxide nanoparticles [NiO] by hydrothermal method.

A 2.4 g of  $\text{Ni}(\text{NO}_3)_2 \cdot 6\text{H}_2\text{O}$  (as a precursor) was dissolved in 30 mL of deionized water to make a 0.5 M solution (1st), and 0.2 g of NaOH was dissolved in 10 mL of deionized water to make a 0.5 M solution (2nd). Then, the same steps in section 2.2.1. were followed

### 2.2.3 Synthesis of titanium dioxide nanoparticles [ $\text{TiO}_2$ ].

Using solvents such as distilled water, isopropanol, and titanium tetra isopropoxide (as a precursor). Titanium tetra isopropoxide [TTIP] and isopropanol were added to 10 mL of distilled water in a 1:4 molar ratio after which a suspension solution of a white color developed. The mixture was then heated to 150 °C for 18 hrs. with a heating rate of 2°C/min, the solution was put into a Teflon linear autoclave cell for hydrothermal synthesis. Once the autoclave is reached the room temperature, the Supernatant was removed, and the precipitates were washed repeatedly with distilled water.  $\text{TiO}_2$  nanoparticles were dried at 90 °C.

### 2.2.4 Synthesis of nanocomposite [ $\text{TiO}_2$ ; CoO/paraffin] by Ultra-sonic method.

The researchers prepared two separate nanoparticle solutions for the study. First, 0.05 mg of cobalt oxide nanoparticles were dissolved in 20 mL of deionized water, resulting in a 0.00005 M solution. Second, 0.05 mg of titanium dioxide nanoparticles were also dissolved in 20 mL of deionized water, creating another 0.00005 M solution. The organic matter of paraffin (0.9 mg) was dissolved in 50 mL of chloroform solvent at ratio of (1:9, metal: paraffin wax). Each solution of nano metal oxide was added slowly (as drops) to the solution of paraffin, then the mixture was ultrasonically irradiated with a high-density ultrasonic probe inglorious straight into the solution under various conditions (40°C, 1h). Sonication time was changed to amplitude in the optimum condition. The precipitate was formed and dried at 90°C in the oven for 5hrs (Figure- 1).

### 2.2.5 Synthesis of nanocomposite [ $\text{TiO}_2$ ; NiO/paraffin] by Ultra-sonic method.

Accordingly, the nanoparticles of nickel oxide (0.05mg) wear dissolved in 20 mL of deionized water (0,00005 M), and nanoparticles of Titanium oxide (0.05mg) were dissolved in 20 mL of deionized water (0,00005 M), while the organic matter of paraffin (0.9mg) was dissolved in 50 mL of chloroform solvent for ratio (1:9, metal: paraffin wax). The same steps in section 2.2.4. were repeated (Figure 2).



**Figure 1:** synthesis of nanocomposites [ $\text{TiO}_2$ ; CoO/paraffin]



**Figure 2:** synthesis of nanocomposites [ $\text{TiO}_2$ ; NiO/paraffin].

### 2.2.6 Preparation Dye-Sensitized Solar Cell(DSSCs).

#### 2.2.6.1 Preparation of (ITO/TiO<sub>2</sub> ; CoO-Paraffin) Photo anodes

To prepare an active anode, 0.1 mg of [TiO<sub>2</sub>; CoO/paraffin]. nanoparticles were dispersed in 10 mL of deionized water (0.00001 M) along with a few drops of diluted acetic acid, and the mixture was agitated for 10 minutes. To achieve a uniform layer thickness and a (2 x 1.5) cm<sup>2</sup> active area, the TiO<sub>2</sub>; CoO/paraffin paste is applied, distributed, and then covered on the four sides of the indium tin oxide conductive glass (ITO glass). After that, the material was dried at room temperature for 30 minutes, put in a furnace for 60 minutes, pulled out to cool, and then washed with water and ethanol. [ITO/TiO<sub>2</sub>; NiO/paraffin] photo anodes are prepared using the same process.to prepare other photo anodes of [ITO/TiO<sub>2</sub>;NiO/paraffin].

#### 2.2.6.2 Preparation of Pt/ITO Cathodic Electrodes

A chemical deposition method is used to deposit platinum Pt on ITO conductive glass in order to create a Pt counter electrode. Drops of chloroplatinic acid (5 mM) are added to the glass, which is then heated at 400 °C for 30 minutes before cooling to room temperature. before cooling to room temperature. By adding a few drops of iodide electrolyte to ITO/TiO<sub>2</sub> and [TiO<sub>2</sub>;CoO/paraffin] placed on ITO glass, which served as the photo-anode, the DSSCs were assembled. A hot melt gasket was used to link the two electrodes face to face. The DSSC's parts were set up in a sandwich-like arrangement.

## 3.Results and Discussion

### 3.1 Characterization

#### 3.1.1 (FT-IR) spectral data for nanocomposite [TiO<sub>2</sub>;CoO/paraffin] by Ultra-sonic method .

FT-IR spectroscopy is an effective method for identifying unknown specimens, providing valuable insights into the molecular composition and chemical bonding of both inorganic and organic materials. The various absorption peaks in the FT-IR spectrum, which are associated with the production of atomic bonds and particular frequencies, provide molecular information about the material as [NiO/paraffin] [5].

The FT-IR spectrum of nanocomposite (see Figure -3). shows bands at 2900cm<sup>-1</sup> (vibratory stretch of C-H group), 1629 cm<sup>-1</sup> (vibration C=C ), 1465 cm<sup>-1</sup> (CH<sub>3</sub> scissoring motion) and 1058 cm<sup>-1</sup> (C-O-C vibration of the skeletal pyranose ring of cobalt oxide) [6,7] and The characteristic band of nano CoO is found to be lightly shifted to the lower frequency at 588 cm<sup>-1</sup>, the additional characteristic band of nanoparticles TiO<sub>2</sub> [8] is found to be lightly shifted to the high frequency at 619cm<sup>-1</sup>, and the paraffin wax shows a band is found at 2920 cm<sup>-1</sup>.

#### 3.1.2 (FT-IR) spectral data for nanocomposite [TiO<sub>2</sub>;NiO/paraffin]by Ultra-sonic method

The FT-IR spectrum of nanocomposite is shown in (see Figure -4). the bands at 3639 cm<sup>-1</sup> (the vibratory stretch of OH), 2956, 2916, and 2850 cm<sup>-1</sup> (stretching vibration of C-H group), 1629 cm<sup>-1</sup> (vibration C=C ), 1465 cm<sup>-1</sup> (CH<sub>3</sub> scissoring motion) and 1114 cm<sup>-1</sup> (C-O-C stretch vibration) were observed. The characteristic band of nanoparticles NiO is found lightly shifted to the lower frequency at 541 cm<sup>-1</sup>, where additional characteristic band of nanoparticles TiO<sub>2</sub> is found lightly shifted to the high frequency at 619cm<sup>-1</sup>, and the paraffin wax Show band at 2918cm<sup>-1</sup>.

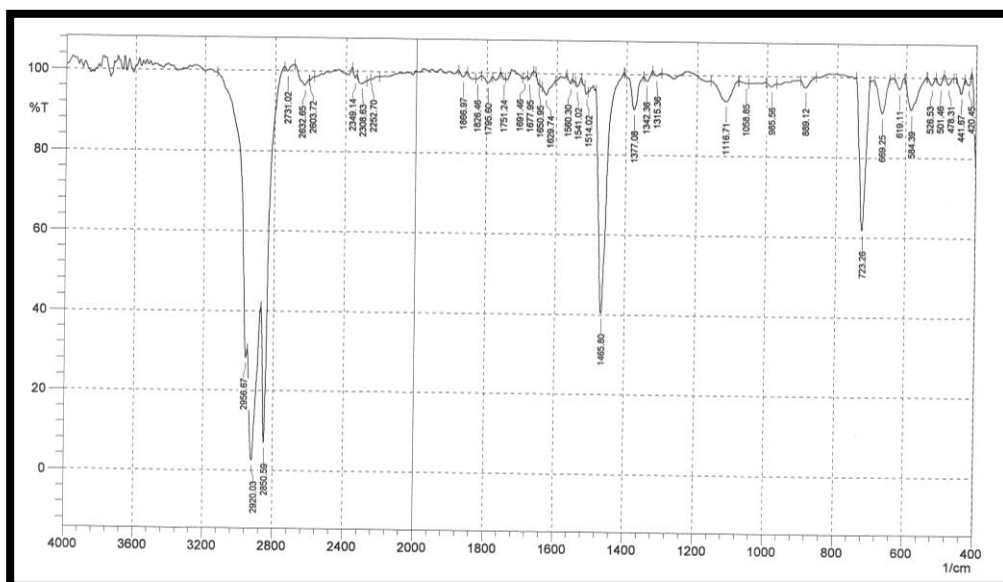


**Figure 3:** (FT-IR) Spectrum for nanocomposite [TiO<sub>2</sub>;CoO/paraffin] by ultra-sonic method.

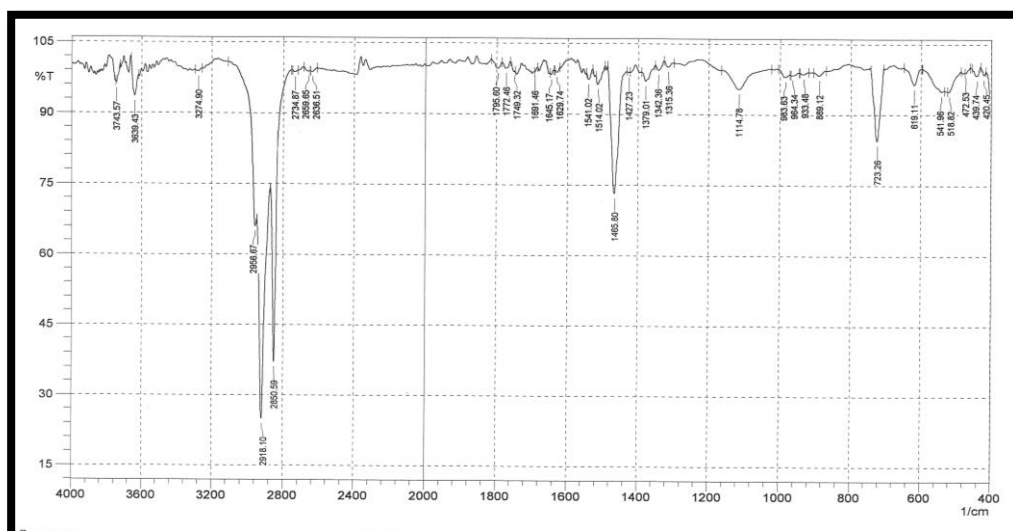


**Figure 4:** (FT-IR) Spectrum for nanocomposite [TiO<sub>2</sub>;NiO/paraffin] by ultra-sonic method.

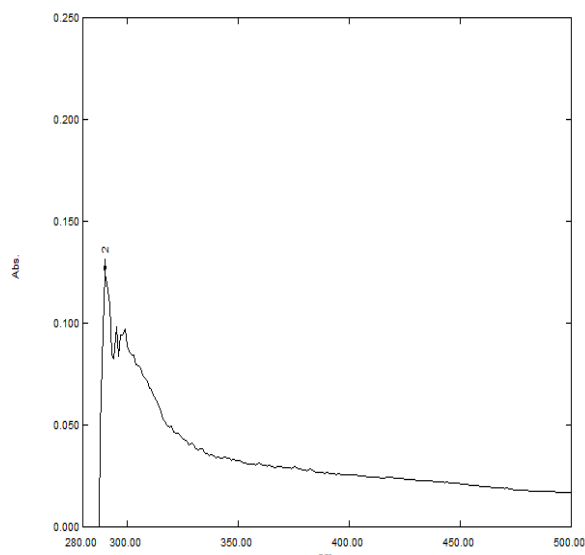
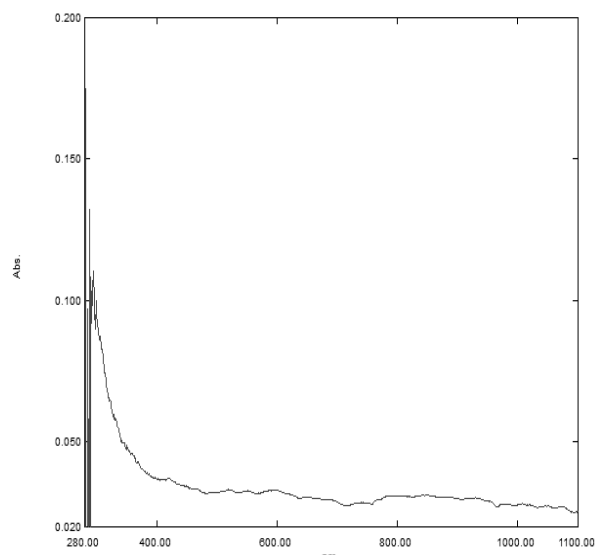
### 3.1.2 UV-Visible Spectroscopy

The theory of UV-visible radiation (the primary method of spectroscopy) is the absorption of ultraviolet or visible light by chemical substances, which generates distinctive spectra. The basis of spectroscopy is the interaction between light and matter. The absorbance spectrum of a substance in solution is obtained using ultraviolet-visible spectroscopy, electrons in a compound or material are stimulated from their ground state to their first singlet excited state by the absorption of electromagnetic radiation or light energy.

The absorbance and wavelengths for all synthesized nanocomposite were measured in chloroform at room temperature. The results are listed in (Table- 1).

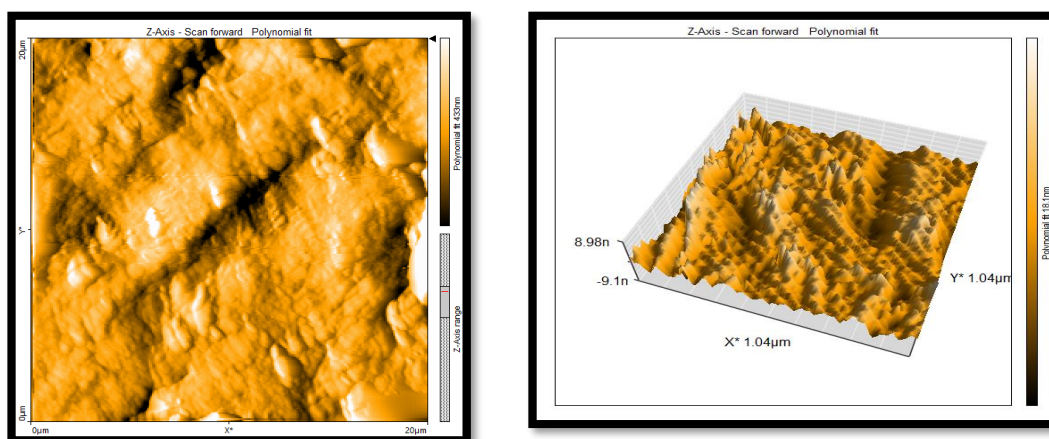
**Table 1:** The absorbance and wavelength for all synthesized nanocomposites

compounds	Wavelength(nm) (Band position)	Absorbance
[TiO <sub>2</sub> ;CoO/paraffin]	931.00	0.011
	290.00	0.124
[TiO <sub>2</sub> ;NiO/paraffin]	270.00	2.551
	227.00	1.929

**Figure 5:** (UV-Vis) spectrum for nanocomposite [TiO<sub>2</sub>;CoO/paraffin] by ultra-sonic method.**Figure 6:** (UV-Vis) spectrum for nanocomposite [TiO<sub>2</sub>;NiO/paraffin] by ultra-sonic method.

### 3.1.3 Atomic force microscopy (AFM) for nanocomposite by The Ultrasonic method.

Two-dimensional (2D) and three-dimensional (3D) atomic force microscopy (AFM) micrographs of nanocomposites comprising paraffin and mixed metal oxides, where the paraffin and metal oxides (Co, Ni) indicate the topography, particle distribution, and average diameter of all the nanocomposites created by the chemical process (ultrasonic technique), which are as follow: the composite [TiO<sub>2</sub>; CoO/paraffin] nanostructure showed that the average diameter of the particles was 87.54 nm (see Figure-7) and the composite [TiO<sub>2</sub>;NiO/paraffin] nanostructure showed that the average diameter of the particles was 56.74 nm (see Figure 8).

**Figure 7:** (2D&3D) AFM images of nanocomposite [TiO<sub>2</sub>;CoO/paraffin].



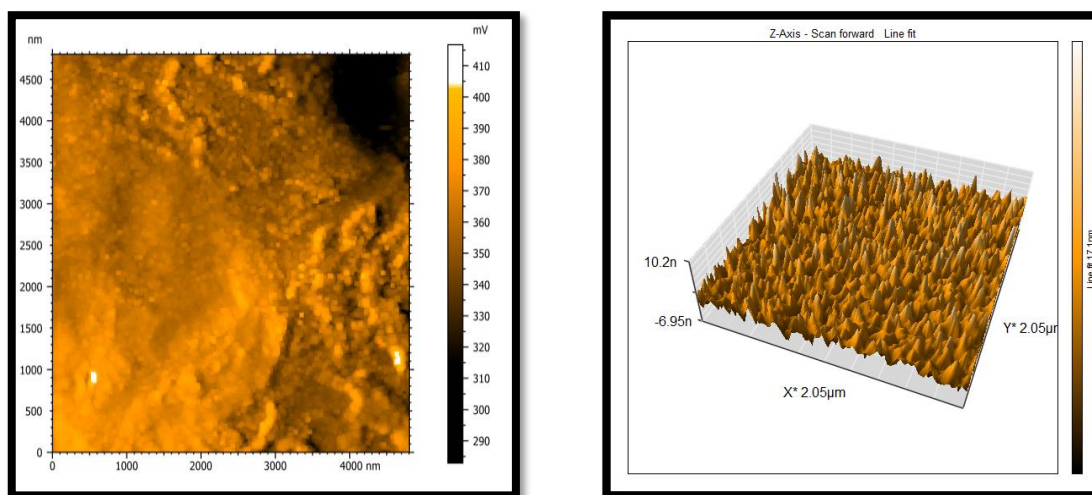


**Figure 8:** (2D&3D) AFM images of nanocomposite  $[\text{TiO}_2;\text{NiO}/\text{paraffin}]$ .

### 3.2.4 Field emission scanning electron microscope with energy dispersive spectroscopy (FESEM-EDS).

The morphology of the surface of the produced material can be studied well with the FESEM. The method of scanning a material with a concentrated electron beam, creates pictures of the subject. When the probe makes contact with the sample surface at the atomic level, a signal is created that contains information about the material's surface characteristics and composition. This signal is generated through interactions between the probe and surface atoms/electrons [9]. The morphology of all the synthesized composites was investigated by FESEM, EDS techniques (see Figure 9) the  $[\text{TiO}_2;\text{CoO}/\text{paraffin}]$  composite image along with mapping its components. The FESEM for  $[\text{TiO}_2;\text{CoO}/\text{paraffin}]$  shows fine particles, And the mapping images show the visual gathering of cobalt, oxygen and titanium above the surface of paraffin. The EDS spectrum shows a peak for oxygen at 11.35%, carbon at 86.19%, titanium at 0.58% and cobalt at 1.88%. (see Figure-10) the  $[\text{TiO}_2;\text{NiO}/\text{paraffin}]$  composite image along with mapping its components. The FESEM for  $[\text{TiO}_2;\text{NiO}/\text{paraffin}]$  shows fine particles, And the mapping images show the visual gathering of nickel, oxygen and titanium above the surface of paraffin. The EDS spectrum shows a peak for oxygen at 12.95%, carbon at 82.60%, titanium at 0.50% and nickel at 3.95%. According to FISEM, the metal oxide nanoparticles are collected in the form of cluster balls on the paraffin surface.

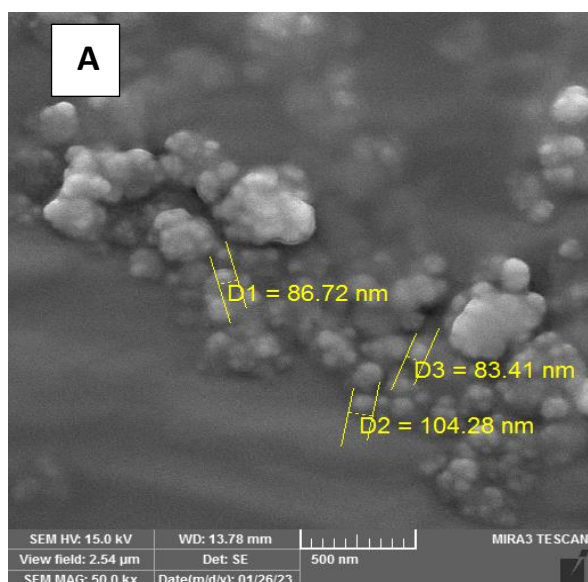


**Figure 9:** Surface morphology of nanocomposite [TiO<sub>2</sub>;CoO/paraffin]: (A) enlargement clip of [TiO<sub>2</sub>;CoO/paraffin]

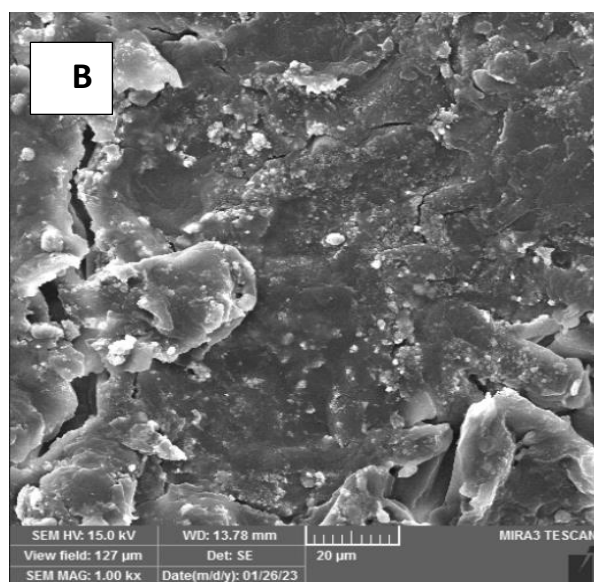


**Figure 9:** (B) SEM image offline crystal of [TiO<sub>2</sub>;CoO/paraffin]

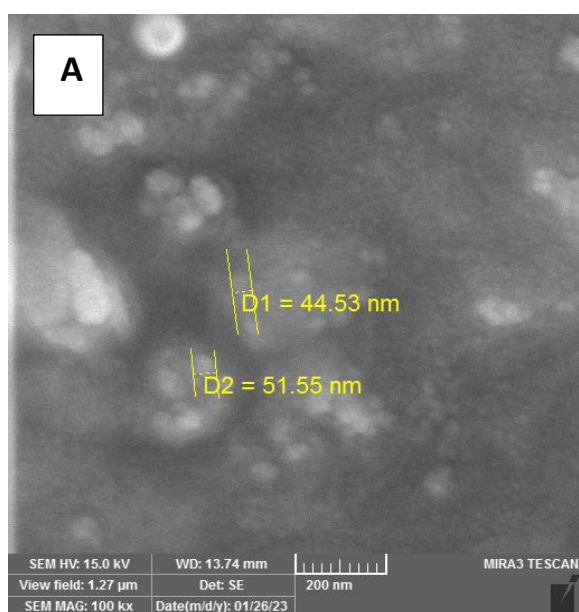


**Figure 10:** Surface morphology of nanocomposite [TiO<sub>2</sub>;NiO/paraffin]: (A) enlargement clip of [TiO<sub>2</sub>;NiO/paraffin]

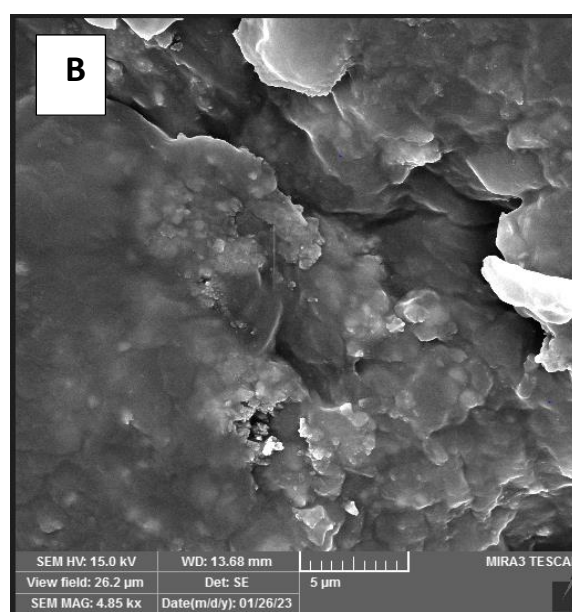


**Figure 10:** (B) SEM image offline crystal of [TiO<sub>2</sub>;NiO/paraffin]

### 3.2.5 X-Ray diffraction of nanocomposite by Ultra-sonic method.

X-ray diffraction is currently a popular method for examining atomic distances and crystal structures. A crystalline sample interacts positively with monochromatic X-rays to create X-ray diffraction, which is based on this interaction using the Denuded - Scherer formula [10]:

$$D = K\lambda / \beta \cos(\theta) \quad \dots\dots\dots(1)$$

**Where:**

**D** = the mean size(nm) of the ordered (crystalline).

**β** = Full width at half maximum (FWHM).

**θ** = angle (in radians).



$\lambda = 0.1541 \text{ nm}$  (the X-ray wavelength).

$K = (\text{constant}) (0.9)$ .

The XRD pattern of the  $[\text{TiO}_2;\text{CoO}/\text{paraffin}]$  nanostructure (Figure 11) exhibits diffraction peaks at  $2\theta$  values of  $23^\circ$ ,  $32^\circ$ ,  $38^\circ$ ,  $40^\circ$ ,  $43^\circ$  and  $63^\circ$  corresponding to the (012), (104), (006), (113), (202) and (300) planes respectively, which are consistent with the  $[\text{TiO}_2;\text{CoO}/\text{paraffin}]$  nanostructure. Crystalline phase Rhombohedral standard JCPDS card number (00-015-0866). However, the mean particle size for  $[\text{TiO}_2;\text{CoO}/\text{paraffin}]$  nanoparticles has a crystal size of 27.86nm.

XRD pattern of  $[\text{TiO}_2;\text{NiO}/\text{paraffin}]$  nanostructure (see Figure-12) the peaks are to  $[\text{TiO}_2;\text{NiO}/\text{paraffin}]$  where exhibited diffraction peaks at the  $2\theta$  values ( $24^\circ$ ,  $33^\circ$ ,  $35^\circ$ ,  $38^\circ$ ,  $41^\circ$ ,  $49^\circ$ ,  $57^\circ$ ,  $64^\circ$ , and  $69^\circ$ ) which are assigned To planes (012), (104), (110), (015), (021), (024), (018), (300), and (208) respectively. Crystalline phase Rhombohedral, standard JCPDS card number (00-033-0960). However, the mean particle size for  $[\text{TiO}_2;\text{NiO}/\text{paraffin}]$  nanoparticles has a crystal size of 25.61nm.

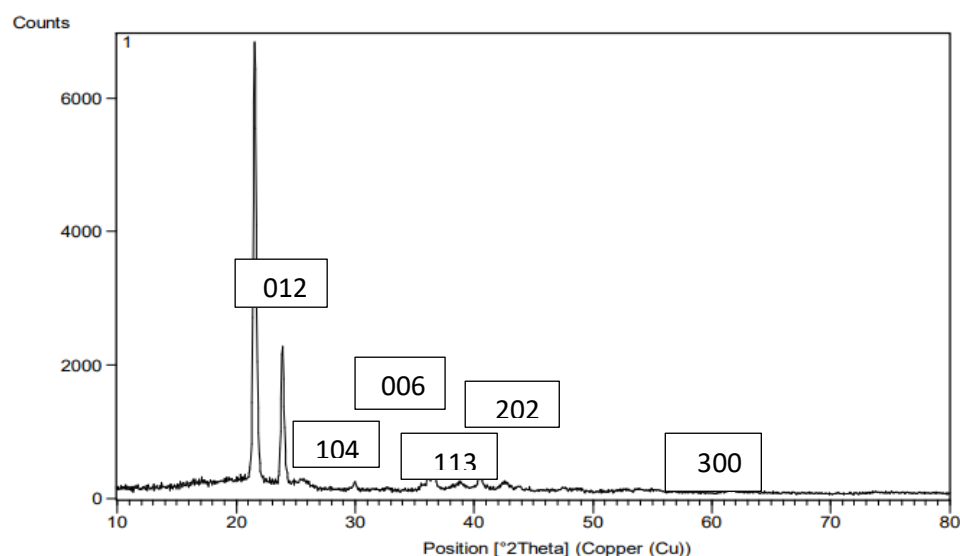


**Figure 11:** XRD pattern of  $[\text{TiO}_2;\text{CoO}/\text{paraffin}]$  nanostructure by ultra-sonic method.

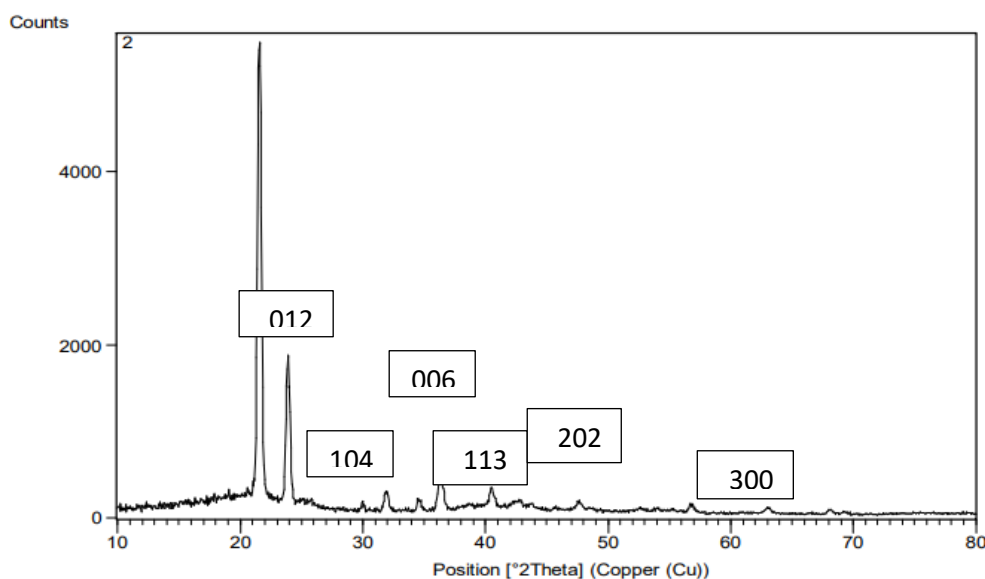


**Figure 12:** XRD pattern of  $[\text{TiO}_2;\text{NiO}/\text{paraffin}]$  nanostructure by ultra-sonic method.

### 3.3APPLICATIONS

#### 3.3.1- Solar cell energy

##### *Fabrication of Dye-Sensitive Solar Cells (DSSCs)*

The general components of DSSCs are dye-sensitizing [ITO/TiO<sub>2</sub>; CoO/paraffin], photo-anodes based on metal oxide-doped paraffin (MxOX-P), [ITO/TiO<sub>2</sub>; NiO/paraffin] electrodes, counter electrodes, and electrolyte solution were made and assembled in a sandwich-like form (see Figure 13).

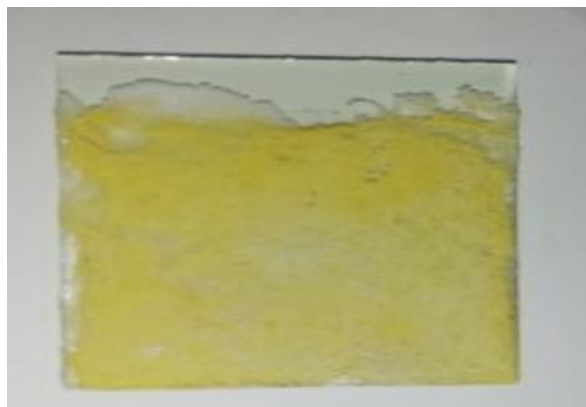


**Figure 13:** One of photo anode electrodes of nanocomposites after immersing in dye.

**Table 2:** Calculated energy conversion (PCE %) and full factor (*ff*) of DSSCs using ITO/[TiO<sub>2</sub>;CoO/paraffin] , ITO/[TiO<sub>2</sub>;NiO/paraffin].

Cells	Voc/V	Isc/A	Vmax/V	Imax/A	FF	P max/w	PCE%
[TiO <sub>2</sub> ;CoO/paraffin]	0.043	0.0001109	0.0250	0.000071280	0.3735	0.000001782	1.7820
[TiO <sub>2</sub> ;NiO/paraffin]	0.006	0.0003000	0.0032	0.000016781	0.2432	0.000000537	0.1075

Table 3 demonstrates that paraffin wax serves as both a phase change material and a heat transfer fluid in this thermal storage system application. This storage mechanism facilitates the simulation of continuous heat energy flow. An approach to estimating storage system efficiency. The efficiency can be increased by using different metal oxides as nanoparticles to enhance paraffin wax to achieve the best heat storage, thermal conductivity, and thermal stability.

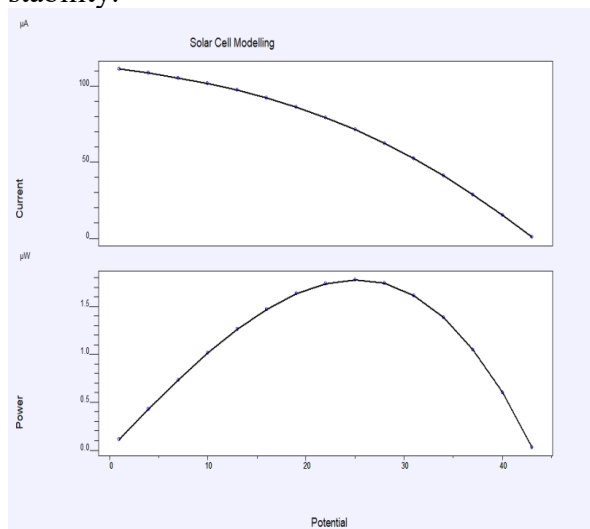


**Figure14:** I-V characteristic of DSSC using ITO/[ TiO<sub>2</sub>;CoO/paraffin].

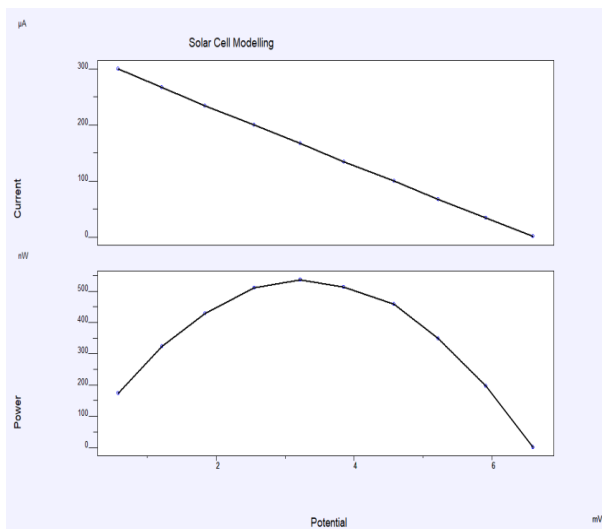


**Figure 15:** I-Vcharacteristic of DSSC using ITO/[TiO<sub>2</sub>;NiO/paraffin].

### 3.3.2 anti-Corrosion

Corrosion is the destructive attack of a metal by its reaction with the environment, depending on how a given metal is used, a wide range of distinct ecosystems may be available. The situation where a bulk aqueous solution makes up the environment is the most typical. Although the aqueous solution in atmospheric corrosion is a condensed thin layer as opposed to a bulk solution, the general principles remain much the same [11].

**Table 3 :** Corrosion characteristics for various compounds and blanks (HCl) solutions.

Comp.	E corr.	I corr.	I corr./ r	Resis.	Anodic $\beta$	Cathodic $\beta$	Corr. rate,	IE%
Blank	-0.527	163.5	3.269E-4	143.2	0.126	0.094	1.605	-
(TiO <sub>2</sub> ;paraffin/CoO)	-0.595	19.11	3.822E-5	4444	0.396	0.386	0.188	88
(TiO <sub>2</sub> ;paraffin/NiO)	-0.544	16.41	3.282E-5	3230	0.185	0.359	0.161	90

The results suggest enhanced corrosion resistance of the paraffin/metal oxide composite. This result is brought about by the metal's high metal affinity, which makes metal oxidation simple and creates a solid barrier to the surfaces of nanocomposites films. Overall findings show that higher metallic nano oxide concentrations in the film were associated with increased corrosion protection efficacies.

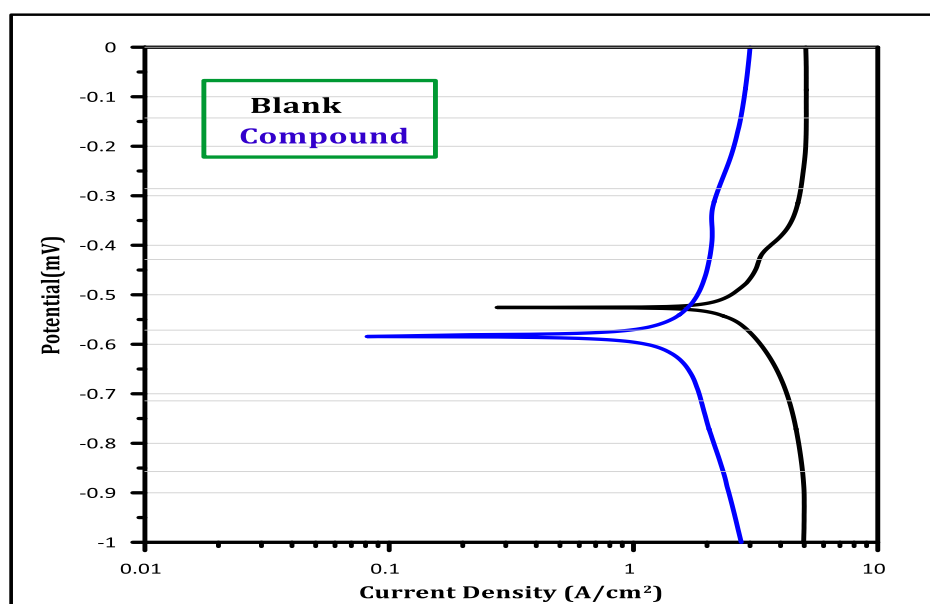


**Figure 16:** Polarization curves for corrosion of blank HCl solution and (TiO<sub>2</sub>;paraffin/CoO).

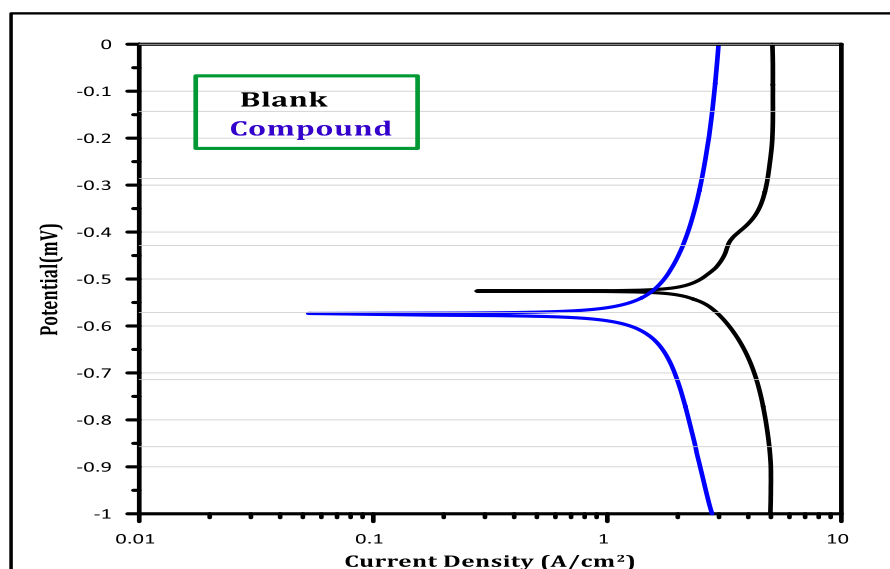


**Figure 17:** Polarization curves for corrosion of blank HCl solution and (TiO<sub>2</sub>;paraffin/NiO).

### Conclusion

In this study, the metal oxide nanoparticles were prepared via a hydrothermal synthesis method, and the nanocomposites were subsequently fabricated using an ultrasonication method. These nanocomposites were examined with different techniques and the preparation of dye-sensitized solar cells. The results of AFM for nanostructures prepared by the ultrasonic method were (87.54nm), (56.74nm), respectively. For nanocomposites, the absorbance spectra of a substance in solution are obtained using ultraviolet-visible spectroscopy at room temperature at the wavelength (850.00, 601.00, 270.00, 227.00 nm). The XRD results mean particle size for [TiO<sub>2</sub>;CoO/paraffin] nanoparticles has a crystal size of 27.86nm and [TiO<sub>2</sub>;NiO/paraffin] nanoparticles has a crystal size of 25.61nm. The industrial applications of the synthesized nanocomposites were investigated, focusing on their potential in solar cell energy production and their efficacy as corrosion inhibitors. The findings for all of these nanocomposites revealed they have the properties of solar cells and a significant inhibitory effect.

### References

- [1] J. Wang and S. Kaskel, " KOH activation of carbon-based materials for energy storage, " *Journal of Materials Chemistry*, vol. 58 ,pp .35-37 ,2012.
- [2] S .Wang, C. Xiao and Y. Xing, " Carbon nanofibers/nanosheets hybrid derived from cornstalks as a sustainable anode for Li-ion batteries, " *Journal of Materials Chemistry*, vol. 44, pp.37-38, 2015.
- [3] Z. Abdin , M. Alim , A. Saidur , R. Islam and M. R. Rashmi, "Solar energy harvesting with the application of nanotechnology," *Journal of Renewable and Sustainable Energy*, vol. 26,pp. 837–852 ,2018.
- [4] I. Manouchehri , P. Kameli and H. Salamati , " Facile Synthesis of Co<sub>3</sub> O<sub>4</sub> /CoO Nanoparticles by thermal treatment of ball-milled precursors," *Journal of Superconductivity and Novel Magnetism* ,vol.24,pp.1907-1910,2016
- [5] A. Ghaffari , M. Behzad, M. Pooyan, M. Amiri , H. Rudbari and G. Bruno, " Crystal structures and catalytic performance of three new methoxy substituted salen type nickel(II) Schiff base complexes derived from meso-1,2-diphenyl-1,2-ethylenediamine, " *Journal of Molecular Structure* ,vol.1063,pp.1–7 ,2014.
- [6] A. Ourari , Y. Ouennoughi , D. Aggoun, M.S. Mubarak, E.M. Pasciak and D.G. Peters, "Synthesis, characterization, and electrochemical study of a new tetradentate nickel(II)-Schiff

- base complex derived from ethylenediamine and 50 -(N-methyl-Nphenylaminomethyl)-20 – hydroxyacetophenone, " *Journal of Polyhedron research*, vol. 67, pp.59–64 ,2014.
- [7] A.D. Khalaji, " Preparation and characterization of NiO nanoparticles via solid-state thermal decomposition of Ni(II) complex, " *Journal of Cluster Sciences*, vol. 24,pp. 189–195 ,2013.
- [8] D. Nadica, M. Abazovic, M. Comor, D. Dramicanin, S. Jovanovic and M. Jovan, , "Photoluminescence of Anatase and Rutile TiO<sub>2</sub> Particles, " *Journal of Physical Chemistry* , vol.66,pp.66-68, 2006.
- [9] P. Andreeva, V. Stoilov and O. Petrov,"Application of X-ray Diffraction Analysis for Sedimentological Investigation of Middle Devonian Dolomites from Northeastern Bulgaria," *Journal of Geologica Balcanica*,vol.8,pp.11-12, 2011.
- [10] D. L. Graver , "Corrosion Data Survey, Metals Section, " NACE, Houston, TX (1985). (Available as an electronic book as "Corrosion Survey Database" by Knovel Corporation, Norwich, NY, 2002.
- [11] F.A.Al-jubouri and B.I.Al-Abdaly , "Cu-ZnO Nanostructures Synthesis and Characterization," *Iraqi Journal of Science*,vol. 62(3),pp. 708-717,2021.
- [12] H.M.Al-saidi, H.H.Hasan and W.W.Hasan , "Preparation and Characterization of ZnO Nano-Sheets Prepared by Different Depositing Methods," *Iraqi Journal of Science*,vol. 63(2),pp. 538-547,2022.
- [13] D.D. Maki, N.N.Kathem, S.S.Mizher and S.S.Najem , "Use of Nano Chemical Additives to Improve the Properties of Industrial Used Paraffin Wax," *Iraqi Journal of Science*,vol.64,pp. 99-104,2019.
- [14] A. A.S.Jasim , K.Kadhim ,A. Aadim and S.S.N.Rashid, " Optical and Structural Properties of Cobalt Nanoparticles Synthesized by Laser Ablation," *Iraqi Journal of Science*, vol 63(10),pp. 4292-4304,2022.
- [15] I. Q. Kaddou and . K. A. Al-Horani, " Mixtures of beeswax and paraffin their importance in bee culture and their role, " *Baghdad Science Journal*, vol. 2, pp. 533–538, 2021.